Decoding auditory working memory load from EEG alpha oscillations

Yichen Yuan[a,*], Surya Gayet[a], Derk Christiaan Wisman[a], Stefan van der Stigchel[a], Nathan van der Stoep[a, b]

[a] Department of Experimental Psychology, Helmholtz Institute, Utrecht University, Utrecht, The Netherlands

[b]Human Machine Teaming, Defense, Safety, and Security, TNO

Conflict of Interest: None

Word count: 9608

Number of Figures: 5

Number of Tables: 0

*** Correspondence:**

Yichen Yuan

Department of Experimental Psychology, Helmholtz Institute, Utrecht University, Utrecht, The Netherlands

Email: y.yuan@uu.nl

Abstract

Working memory (WM) enables temporary retention of task-relevant information for imminent use. Increases in visual WM load are accompanied by elevated contralateral delay activity (CDA), and EEG alpha-band power. While most WM research focuses on the visual domain, it remains unknown whether similar EEG responses also reflect WM load in the auditory domain. Using EEG, we set out to establish such neuro-markers of auditory WM load. Participants memorized the pitches of 1 to 4 pure tones presented to one ear, with 1 to 4 consistent distractor tones presented to the other ear. Behaviorally, auditory WM capacity plateaued between set-sizes two and three. Unlike for visual WM, auditory WM load was not reflected in lateralized EEG responses. This shows that the CDA is a vision-specific rather than domain-general neuro-marker of WM load. Applying multivariate pattern analyses on the delay activity revealed that auditory WM load is reflected in (mostly temporal) patterns of alpha-band oscillations. Surprisingly, a temporal generalization analysis revealed that the alpha patterns reflecting specific load conditions changed throughout the maintenance period (despite load being inherently constant), revealing dynamic coding of auditory WM load.

Keywords: Auditory working memory, CDA, EEG decoding, Memory capacity, Modality-specific

1 Introduction

Working memory (WM) is a limited-capacity system that allows us to temporarily hold several representations accessible in service of other mental tasks (Cowan, 1998). Commonly, not all task-relevant information is available in one location or at a single moment, which requires us to temporarily retain information in mind. For instance, we may memorize a phone number for subsequent dialing or remembering a list of ingredients while grocery shopping. WM functions as our central information storage-and-processing structure (Cowan et al., 2005), which enables us to interact with the world over space and time.

So far, Baddeley and Hitch (1974) proposed probably the most influential WM model, which comprises three components: (1) a visuo-spatial sketchpad for storage of visual information; (2) a phonological loop for storage of auditory information; (3) a central executive that regulates the content of the active portion of WM. Years later, Baddeley (2000) added a fourth component, the episodic buffer, that binds features from different sources together into multidimensional objects. According to Baddeley's model, the storage of WM is modality-specific, with a visuo-spatial sketchpad for visual information and a phonological loop for auditory information. Indeed, previous studies have provided evidence that visual and auditory WM may rely on at least partly distinct structures that produce dissociable neural responses (Lefebvre et al., 2013; Pratt et al., 1989; also see Scimeca et al., 2018 for sensory recruitment hypothesis).

Given the (at least partly) modality-specific nature of WM, it is reasonable to use modality-specific stimuli to study visual WM and auditory WM separately. Yet, most WM studies to date focused on the visual modality, for instance the color, orientation, spatial location, etc. of visual items (Carlisle et al., 2011; Diamantopoulou et al., 2011; Harrison & Tong, 2009; Li & Saiki, 2015; Luria & Vogel, 2011; Schurgin, 2018). Correspondingly, studies

have found evidence for the existence of a 'magic number four', the observation that visual working memory capacity is severely limited to an average of four items in young adults (Cowan, 2010). By recording electroencephalograms (EEG), Luck and Vogel (1997) identified a neuro-marker of visual WM load and named it Contralateral Delay Activity (CDA). Specifically, they presented a symmetric visual array in which the left and right side differed in features and instructed the participants to memorize the objects in only one hemifield. In this bilateral change-detection paradigm, information presented on both sides was perceptually processed, but information presented in only one hemifield was subsequently retained in WM. Interhemispheric difference waves were calculated for each set-size condition by subtracting the ipsilateral activity from the contralateral activity. By doing so, any nonspecific, bilateral Event-Related Potentials (ERPs) were removed. This approach thus allows to isolate the neural activity specifically related to encoding and maintenance of the memorized objects. A large negative-going voltage over the contralateral hemisphere (relative to memorized hemifield) was observed, located primarily over posterior parietal and lateral occipital electrodes. Moreover, the amplitude of the CDA varied with visual WM load, as it increased between set-sizes of one, two and three items, and then leveling off at the group's average capacity limit of about three items (Vogel & Machizawa, 2004). Interestingly, the existence of lateralized responses to set-size (such as the CDA), imply that visual WM is inherently spatially organized.

Another neural marker of visual WM has been observed in the frequency domain. For instance, Jensen et al. (2002) have shown that the power of oscillations in the alpha-band (8-12 Hz) over the posterior and central EEG channels track visual memory load during the maintenance period. Such increases in alpha band power during WM maintenance are widely accepted as reflecting functional disengagement or inhibition of task-irrelevant visual inputs to protect the task-relevant information maintained in WM (Bonnefond & Jensen, 2012; Roux & Uhlhaas, 2014; Tuladhar et al., 2007; Wianda & Ross, 2019). Taken together, several neuro-

markers of WM load have been established in the visual domain, some of which are lateralized (capitalizing on the spatial organization of visual WM) and some of which are not.

Surprisingly, little is known about auditory WM. In the current study, we define auditory WM as the maintenance of acoustic properties of sound stimuli, such as the pitch, duration, timbre, and amplitude (following Lefebvre et al., 2013). It should be noted that the maintenance of verbal information is not necessarily the same as auditory WM. Studies have found that maintenance of verbal and of purely acoustic material share relatively few characteristics (Deutsch, 1970; Williamson et al., 2010). In the studies focusing on the maintenance of acoustic properties, the auditory WM capacity found in tasks using pure tones was around 2 to 3 (Alunni-Menichini et al., 2014; Li et al., 2013; Prosser, 1995). Lefebvre et al. (2013) set out to identify the neuro-marker of auditory short-term memory. Contrasting the univariate EEG response during the maintenance period between the memory task and a control task revealed a sustained negative-going voltage over the central-frontal electrodes that scaled with auditory WM load. This negativity was identified as a neuro-marker of auditory WM and named as the sustained anterior negativity (SAN). In a follow-up study, Alunni-Menichini et al. (2014) showed that the amplitude of SAN increased in negativity from 2 to 4 items and then levelled off from 4 to 8 items. Thus, they established the SAN as an index of brain activity specifically reflecting the amount of information (load) maintained in auditory WM. In these studies investigating auditory WM, however, stimulus presentation was not lateralized, unlike typical visual WM studies measuring lateralized responses (CDA). Thus, it remains unknown whether lateralized responses that hinge on the inherently spatial organization of WM (akin to the CDA for visual WM) can also be observed for auditory WM load.

Other studies, focusing on the frequency domain of the EEG response, have found that alpha oscillations (8-12 Hz) are also a sensitive marker for auditory WM load (Kaiser et al., 2007; Leiberg et al., 2006; Luo et al., 2005; Van Dijk et al., 2010). For instance, Leiberg et al.

(2006) found monotonic increases in spectral amplitude as a function of memory load for the alpha band over right frontal sensors during the delay period. Similarly, Van Dijk et al. (2010) also found a left-lateralized (left temporal regions) increase in 5-12 Hz during the maintenance of pitches, compared to a non-memory control task. Alpha-band oscillations can therefore be considered to reflect the maintenance of auditory information. Earlier work has interpreted alpha-band oscillatory responses to either reflect the top-down control of a WM representations (Leiberg et al., 2006) or the inhibition of task-irrelevant neural processes (Van Dijk et al., 2010). Either way, alpha-band oscillatory responses are closely related to maintenance of auditory information (for a review, see Wilsch & Obleser, 2016), and may therefore track auditory WM load.

Recently, multivariate pattern analysis (MVPA) has been advocated in the study of higher order brain states, as it is more sensitive to pick up on complex scalp patterns of neural activity, compared to univariate methods (Kikumoto & Mayr, 2018; Peelen & Downing, 2023). While most WM decoding studies have focused on visual representations, less is known about the maintenance of auditory stimulus features. A handful of multivariate fMRI studies have shown that auditory information (e.g., frequency, location, etc.) can be decoded in auditory (Linke et al., 2011), inferior frontal (Kumar et al., 2016), precentral cortex (Uluç et al., 2018), and superior parietal lobule (Czoschke et al., 2021). Moreover, we are not aware of any study using multivariate analyses to investigate executive properties (such as load) of or auditory WM. Thus, in the present study we set out to uncover the spatio-temporal patterns of EEG activity relating to auditory WM load.

Considering the large knowledge gap between what we know about visual WM and auditory WM, it seems imperative to study auditory WM via various methods (especially multivariate methods) used in visual WM literatures. Moreover, previous studies into auditory WM have only used binaural stimuli, where potential lateralized (i.e., contralateral-minus-

ipsilateral) responses akin to the CDA would remain unnoticed. It therefore remains unknown whether the CDA is a modality-specific neuro-marker for visual WM or whether it is a supra-modal neuro-marker that also reflects auditory WM load. In the current study, we aimed to identify load-dependent neuro-markers of auditory WM by recording EEG signals. Specifically, we asked two research questions, namely, (1) whether auditory WM load is reflected in lateralized neural responses, akin to the CDA for visual WM load, and (2) whether we could identify non-lateralized load-dependent neuro-markers of auditory WM, using multivariate pattern analyses.

To address these questions, we conducted an auditory delayed change-detection task (e.g., Rouder et al., 2011) while recording EEG. On each trial, participants memorized a tone sequence comprising 1, 2, 3, or 4 pure tones differing in pitch, thus yielding four set-sizes. Importantly, this auditory change-detection task was combined with a dichotic listening task (e.g., Hugdahl, 2011), whereby the to-be-memorized tone sequences were presented to one ear, while a to-be-ignored distractor sequence was presented to the other ear. Participants were instructed to memorize the tones presented to one ear, while ignoring the tones presented to the other ear. After a delay period, a probe sound was presented to the attended ear, with a distractor presented to the un-attended ear. Participants were required to indicate whether the probe was present or absent in the memory tone sequence. This dichotic listening approach allowed us to isolate load-dependent and hemisphere-specific EEG responses during the delay period of the auditory WM task. By doing so, we could compute the contralateral-minus-ipsilateral response differences, and compare these between set-size conditions to identify potential lateralized load-depended neuro-markers of auditory WM (akin to the CDA).

We analyzed the EEG data using both univariate and multivariate methods (EEG and decoding), investigating lateralized and non-lateralized responses, in the time and frequency domain. EEG responses are retrieved from the maintenance period, when participants held

varying numbers of pitches (i.e., set-sizes) in auditory WM. For behavioral performance, we expected that the estimation of WM capacity should increase with set-size, levelling off at the WM capacity limit. For the univariate EEG results, we focused on lateralized responses, namely the CDA responses and lateralized alpha oscillations, based on previous visual WM studies (Jensen et al., 2002; Vogel & Machizawa, 2004). If auditory WM is also reflected in lateralized responses, the contralateral-minus-ipsilateral univariate responses and alpha-band power should scale with auditory WM set-size (until it levels off at the WM capacity limit). For multivariate pattern analysis, we focused on decoding scalp patterns of alpha-band (8-12 Hz) power, based on previous findings that alpha was closely related to auditory WM (Leiberg et al., 2006; Wilsch & Obleser, 2016). If the patterns of alpha oscillation during the maintenance period indeed track auditory WM load, the alpha oscillation patterns should be distinguishable between load conditions up to the group-level capacity limitations, but fail to differentiate among conditions that exceeded this limit, as reflected in the auditory WM capacity calculated by the behavioral data.

To preface the results, we found that auditory WM load was not reflected in lateralized responses, neither in the time nor in the frequency domain. This implies that the CDA is vision-specific rather than domain-general marker of WM load. Our decoding results showed that patterns of alpha-band oscillations during the maintenance period reflected auditory WM load. Decoding was predominantly driven by (bilateral) temporal electrodes. Moreover, the alpha patterns associated with specific load conditions were changing throughout the maintenance period, which suggests that auditory WM load is reflected in dynamic – rather than static – neural population codes. Mirroring the behavioral data that the auditory WM capacity is around 2 tones, these load-specific EEG responses allowed to distinguish between load conditions within, but not beyond, the group-level capacity limitations. We thus consider scalp patterns of alpha band power as a novel neuro-marker for auditory WM load.

2 Materials and Methods

2.1 Participants

To determine the required sample size for a main effect of set-size in our within-participants design, a sample size estimation was performed in G*power software (Faul et al., 2009). This suggested that at least 19 participants were required for 85% power to observe a medium effect size (Cohen's f = .3) with a repeated measure ANOVA (α = 0.05). A total of 27 participants were tested (18 participants reported their gender as female, 9 as male; mean age = 22.41 years, SD = 1.91, range = 19 to 25 years). We stopped testing after enough participants (>19) met our inclusion criteria for the EEG analyses (for details, see the EEG recording section below). All participants reported normal or corrected-to-normal vision and normal hearing (as tested with a pre-experiment audiogram). They signed informed consent and received money or course credits for their participation. The study protocols were approved by the faculty ethics committee (FETC) of Utrecht University (number 18-048 van der Stoep).

2.2 Apparatus and stimuli

The experiments were conducted in a dimly lit lab and controlled using Matlab 2018a. Participants were seated with their head positioned in a chin rest, to keep their viewing distance at a fixed 60 cm in front of a 27-inch monitor. The auditory stimuli were played through 3M™ E-A-RTONE™ Insert Earphone 3A (10 Ohm).

The auditory stimuli consisted of 25 pure tones with different frequencies and white noises, each lasting for 200 ms. All sound were generated in Matlab 2018a, sampled at 96 kHz. The frequencies of the 25 target pure tones ranged from 125 Hz to 8.1 kHz with a 19% increase in-between tones (125, 149, 177, 211, 251, 298, 355, 422, 503, 598, 712, 847, 1008, 1200, 1428, 1699, 2021, 2406, 2863, 3407, 4054, 4824, 5740, 6831, 8129 Hz), which should be

distinguishable for naive listeners (Ahissar et al., 2006). The lowest (125 Hz) and highest (8129 Hz) frequency from this set of pure tones were used as distractors, while the remaining 23 pure tones were used as the set of target stimuli. Linear ramps of 25 ms were applied both to the beginning and the end of tones to prevent auditory pop artifacts. Participants were able to slightly adjust the volume to a subjectively comfortable level at the start of the WM tasks. Sounds were on average presented at 60 dB(A).

2.3 Procedure

Pitch discrimination task

To make sure that participants could distinguish different pure tones, a behavioral pitch discrimination task was conducted before the main auditory WM task. In this pitch discrimination task, every tone in the pre-generated 25 pure tone set was paired with itself, and the adjacent tones (i.e. one higher frequency for the lowest tone, one lower frequency for the highest tone, and one lower and one higher frequency for the tones in-between), yielding 73 pairs of pure tones. On each trial, one pair of tones was presented bilaterally and sequentially. Participants were required to indicate whether the two tones were the same or different. All pairs were presented once. Accuracies in the task for all participants were higher than 85% (M = 97.2%, *SD* = 2.86%, range = 89% to 100%), indicating that participants could distinguish the different tones; therefore, no participants were excluded based on this criterion.

Auditory WM task

After the pitch discrimination task, participants performed the auditory WM task during EEG recording. In this WM task, a 4 (Set-size: 1, 2, 3, vs. 4) × 2 (Attended side: Left vs. Right) within-participants design was adopted. At the beginning of each trial, participants were always given instructions to remind them of which side to attend to. They were required to memorize the pitches of a sound sequence presented on the attended side, while ignoring the sound

sequence presented on the unattended side. The manipulation of the to-be-attended side was blocked, while set-size varied randomly from trial to trial. The order of blocks was counterbalanced across participants.

On each trial, a fixation cross appeared at the center of the screen for 1000 ms, after which two different sound sequences were presented separately to each ear. These two sequences were presented simultaneously, comprised the same number of pure tones, but differed in pitch. The sound sequence consisted of four sounds, separated by inter-sound intervals. Each sound was either a pure tone or a white noise burst, depending on the experimental condition. The duration of the pure tones, the white noise, and the inter-tone intervals was 200 ms, yielding a sound sequence that consistently lasted for 1400 ms. For the attended side, the last one (set-size 1), two (set-size 2), three (set-size 3), or four (set-size 4) sounds were randomly sampled without replacement from the predefined set of 23 target pure tones, and participants were required to memorize the exact pitches of these pure tones. White noise bursts were used to fill up the sequence where no pure tone was presented (i.e., in set-sizes below 4; see Figure 1). For the unattended side, the last one (set-size 1), two (set-size 2), three (set-size 3), or four (set-size 4) sounds consisted of distractor sounds. The distractor sound was either the lowest (125 Hz) or the highest frequency (8.1 kHz) from the predefined distractor set of pure tones (with equal probability), and was repeated once (in set-size 1 condition), twice (in set-size 2 condition), three times (in set-size 3 condition), or four times (in set-size 4 condition), matching the number of pure tones on the attended side. Similarly to stimulus presentation in the attended side, white noise bursts were used to fill up the sequence of pure tones in the unattended side (i.e., in set-sizes below 4). After the presentation of the sound sequence, a maintenance period of 2000 ms followed, during which participants had to hold the pitches in memory (1 to 4 target sounds). Finally, after the maintenance period, two probe sounds were presented for 200 ms, separately to the attended and unattended side. The probe

sound on the attended side was the test sound, which could either be present (50% trials) or absent (50% trials) in the memorized sound sequence. On target-present trials, the probe sound was randomly selected from the memorized sound sequence with equal probability. On target-absent trials, a tone from the memorized sound sequence was similarly selected, but substituted with an adjacent pure tone (i.e., one step higher or one step lower in the pre-generated target set of 23 pure tones). The sound on the unattended side was the same distractor that was presented in the original sound sequence (125 Hz or 8.1 kHz). After the offset of the probe sound, participants were required to indicate as accurately as possible whether the probe sound on the attended side was present or absent in the memorized sound sequence, while ignoring the sound on the unattended side. After the response (present vs. absent), the next trial started (See Figure 1). Overall, participants completed a total of 416 trials divided into eight blocks; two practice blocks of 16 trials each, followed by six experimental blocks of 64 trials each.

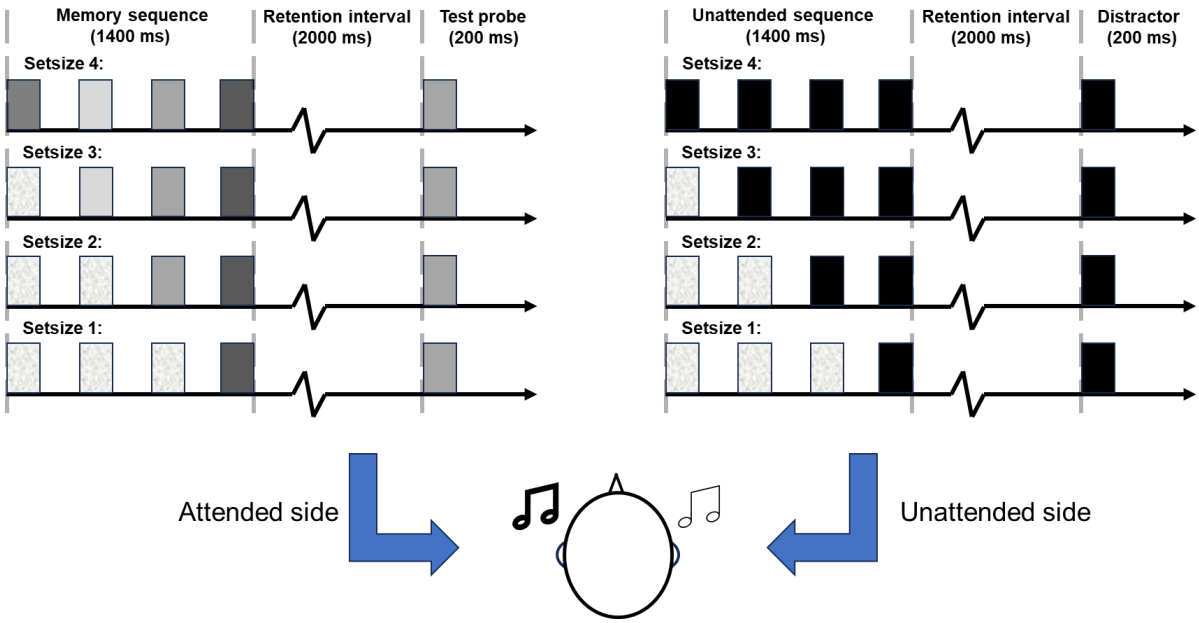

Figure 1. Schematic depiction of the task. Two different sound sequences were presented separately and simultaneously to each ear, whereby the participant was instructed to attend one side and ignore the other. On the attended side, the last 1, 2, 3, or 4 sounds (depending on the set-size) of the sequence were pure tones of different frequencies that participants were

instructed to memorize. On the unattended side, the last 1, 2, 3, or 4 sounds in the sequence consisted of the same (low or high pitched) pure tone, which participants could ignore. On both sides, the remaining (3, 2, or 1) sounds consisted of white noise. After a two second delay, during which participants maintained 1, 2, 3 or 4 sounds in memory, a probe sound was presented to the attended side while the to-be-ignored tone was presented to the other side. Participants were required to indicate whether the probe sound was present or absent in the memorized sound sequence.

2.4 EEG recording

EEG was recorded at a sample rate of 2048 Hz from 32 standard electrode sites placed according to the international 10/20 system using a BioSemi EEG system. Six additional EXG flat type electrodes were used to record horizontal and vertical eye movements and provide mastoid references. During the experiment, participants were instructed to fixate on the center of the monitor and try not to make horizontal or vertical eye movements.

The offline analysis of EEG data was performed using Matlab 2022a (https://www.mathworks.com/) and eeglab 14.1.2b (Delorme & Makeig, 2004). For pre-processing, EEG data were first re-referenced to the average of all 32 channels. Then a 0.01 Hz to 40 Hz band-pass filter and a 50 Hz notch filter were applied to remove high frequency noise and electromagnetic radiation from the environment. After the filtering, EEG data were down-sampled to 256 Hz to speed up computation. Then, an infomax independent component analysis (ICA) algorithm (Bell & Sejnowski, 1995) was applied to correct the signal for eye movement artifacts. The SASICA plugin with ADJUST was used to automatically identify the artifact component (Chaumon et al., 2015). Furthermore, the EEG signals were segmented into 5500 ms epochs (-1000 ms to 4500 ms relative to the onset of the sound sequence) separately

for each attended side and set-size condition. The interval of 0-200 ms prior to the onset of the sound sequence served as baseline. Finally, epochs with voltages exceeding ±200 μV were excluded from further analysis. Six participants were excluded because an excessive number (>25%) of EEG epochs were removed (i.e., voltages exceeding ±200 μV). The average epoch rejection rate of the remaining participants was 6.40% of all trials (*SD* = 6.67%, range = 0-24.7%).

2.5 Behavioral data analyses

Accuracy rate and working memory capacity *K* were calculated separately for each participant in each experimental condition (Equation 1; Rouder et al., 2011). In the equation, *K* is WM capacity, *N* is the number of items in the memory sequence (set-size), and *H* and *F* are the observed hit rates and false alarms in Set-size N condition, respectively. Moreover, participants whose accuracy and WM capacity *K* exceeded ±3 *SD* of the group mean value were removed. This criterion led to exclusion of data from one participant.

$$K = N \times (H - F) \qquad \text{(Equation 1)}$$

Bayesian repeated measures analyses of variance (RM ANOVAs) were conducted separately for mean accuracy and mean auditory WM capacity *K* with factors Set-size (1, 2, 3, vs. 4) and Attended side (Left, vs. Right) using JASP 0.17.3.0 (JASP Team, 2024). The default priors were applied while the seed value was consistently set to 1 for repeatability. Moreover, effects were evaluated across matched models (Mathôt, 2017), by comparing models containing the factor of interest to equivalent models without this factor. This approach provides an "Inclusion Bayes Factor" (BF_{incl}), which reflects the amount of evidence for or against the specific (main or interaction) effect of interest. We followed the guidelines suggested by Kass and Raftery (1995) for the interpretation of Bayes factors. Specifically, BFs

larger than 3 signified substantial (or more) evidence in favor of the effect; BFs between 0.3 and 3 signified no conclusive evidence in favor of or against the effect; BFs smaller than 0.3 signified substantial (or more) evidence against an effect.

2.6 EEG Data analyses

For EEG data analyses, we aimed to answer the following two questions: (1) Is auditory WM load reflected in lateralized neural responses, akin to the CDA for visual WM load? (2) Can we identify non-lateralized load-dependent neuro-markers of auditory WM? To answer question 1, we computed the lateralized (i.e., contralateral minus ipsilateral) EEG response amplitude and the lateralized alpha-band (8-12 Hz) power evoked in the four different set-size conditions. For question 2, we applied multivariate decoding to patterns of alpha-band power across the scalp, as measured during the maintenance period. The focus on alpha-band over other frequency bands followed from previous studies showing close relationship between alpha oscillations and WM maintenance (Leiberg et al., 2006; Wilsch & Obleser, 2016). All data analyses were performed in Matlab with Fieldtrip toolbox (Oostenveld et al., 2011; Donders Institute for Brain, Cognition and Behaviour, Radboud University, the Netherlands. See http://fieldtriptoolbox.org) and MVPA-light toolbox (Treder, 2020)

2.6.1 Lateralized responses in time and frequency domain

To test whether there is an overall lateralized (CDA-like) response (reflecting the instruction to either memorize tones on the left or the right side), contralateral and ipsilateral EEG responses were averaged across all set-size conditions. Then a cluster-based permutation test (paired *t*) (Maris & Oostenveld, 2007) was conducted to test for a difference between the contralateral and ipsilateral EEG responses during the maintenance period (1400 to 3400 ms relative to the onset of the sound sequence). This permutation test was performed on all

lateralized electrodes, to assess which timepoints exhibit a CDA-like response to auditory WM load. The permutation test consisted of four steps: (1) Paired-sample *t*-tests were used to test at each time point and each electrode whether the contralateral and ipsilateral responses differed at the group level. (2) Clusters were defined as contiguous time points for which the *t*-test was significant ($p < .05$) at least at one electrode. Then, for each of these clusters, the *t*-values were summed to obtain a cluster-level *t* mass. (3) We constructed a null distribution of cluster-level *t* mass values, by randomly swapping the condition label (contralateral or ipsilateral) across trials, for each participant, and then calculating the maximum cluster-level *t* mass at the group level. Importantly, labels were swapped for an entire trial (i.e., time-series) rather than timepoint-by-timepoint, to preserve autocorrelations between timepoints in the null data. By repeating this procedure 1000 times, we obtained a null distribution of maximum cluster-level *t* mass values. (4) Finally, we computed *p* values for each of the clusters in the observed data, by computing the fraction of permuted data sets containing *t* mass values at least as extreme as that of each observed cluster (using a two-tailed alpha = 0.05). We considered channels to exhibit a CDA-like response, whenever channels yielded a significant lateralized response throughout the entire cluster.

To test whether the CDA-like response scaled with set-size, we followed the same procedure as above, but for each set-size condition individually. Another cluster-based permutation test was conducted to compare the lateralzied responses across four set-size conditions during the maintenance period (1400 to 3400 ms relative to the onset of the sound sequence). This permutation test was performed on all lateralized electrodes, to assess during which timepoints and for which electrodes the CDA-like response scales with set-size.

A similar approach was followed to test for lateralized load-dependent responses in the time-frequency domain (alpha power). Instead of using the raw (i.e., voltage) EEG responses, a time-frequency analysis was performed first, using 7-cycle Morlet wavelet decomposition

(i.e., $mf_o\sigma_t=7$; Roach & Mathalon, 2008) for frequencies ranging between 4 and 30 Hz in 1 Hz steps. The Morlet filtering was performed by convolving single-trial EEG epochs from each scalp electrode with complex Morlet wavelets. A 7-cycle Morlet wavelet was used in this analysis to provide a good tradeoff between time and frequency resolution. The decomposition was performed on 5.5 s EEG epochs after the pre-processing described above, ranging from -1000 ms to 4500 ms relative to the onset of the sound sequence. After Morlet wavelet decomposition of the trials was performed, oscillatory power was calculated, by taking the square of the modulus of the resulting complex number. Each trial was baseline corrected by subtracting the average power in the window of -200-0 ms before onset of the sound sequence. Following the approach of previous studies, we focused on the power in the alpha frequency band (8-12 Hz) (Leiberg et al., 2006; Wilsch & Obleser, 2016).

Cluster-based permutation testing (following the same procedures as above) was performed to test for the existence of a lateralized alpha response, and to test whether this lateralized alpha response scales with set-size.

2.6.2 EEG decoding analyses

The goal of the decoding analyses was to test for the existence of non-lateralized EEG responses that scale with auditory WM load. Compared to univariate approaches, multivariate decoding is more sensitive to uncover differences between conditions as it leverages the scalp distribution of neural signals, allowing for the detection of discriminable patterns that may not be evident in individual electrodes (Peelen & Downing, 2023). Here, we set out to classify different load conditions based on the scalp distribution of alpha-band power, using the MVPA-light toolbox (Treder, 2020) in Matlab.

We performed two distinct MVPAs to test whether we could distinguish the patterns of

activity evoked by different set-size conditions. First, we trained classifiers to differentiate between set-size conditions by performing timepoint-by-timepoint decoding (i.e., training and testing the classifier on data from the same timepoint within a trial). Six different decoding comparisons (Set-size 1 vs 2, 1 vs 3, 1 vs 4, 2 vs 3, 2 vs 4, 3 vs 4) were performed separately for each time point from the onset of the sound sequence to the end of the maintenance period. Second, we conducted a temporal generalization analysis, whereby classifiers were trained and tested on all possible combinations of timepoints. This temporal generalization analysis allowed us to identify whether the neural response to auditory WM load was stable over time or was dynamically changing during the maintenance period. Here as well, we conducted six different decoding comparisons (Set-size 1 vs 2, 1 vs 3, 1 vs 4, 2 vs 3, 2 vs 4, 3 vs 4). Finally, for both analyses, we also calculated the (absolute) contributions of each electrode to the classifier. The amount of classifier contribution would inform us of which electrodes were most important to obtaining the observed classification performance.

Decoding: timepoint-by-timepoint classification

To test whether scalp patterns of alpha oscillations tracked auditory WM load, we conducted a timepoint-by-timepoint decoding analysis, ranging from the start of stimulus encoding to the end of the maintenance period, using electrodes as features. To obtain the mean alpha-band power, the data was first down-sampled over time by averaging every five consecutive time points (20 ms) without overlap. Then the data was z-scored, and data from each set of 5 consecutive trials within the same set-size condition were averaged to improve the signal-to-noise ratio. This resulted in 35 compound 'trials' (samples) on average (SD = 2.62, range = 28-38) that could be used for our decoding analyses.

We used linear SVM classifiers with a leave-one-trial-out cross-validation procedure to

decode between set-sizes. Taking set-size 1 vs. 2 as an example, we performed classification analyses to investigate whether the scalp pattern of alpha-band power could distinguish between set-size 1 and 2 conditions. Above-chance classification would imply that the patterns of alpha-band power were load-dependent. Specifically, for a given timepoint, and on each cross-validation iteration, one compound trial (i.e., the average of 5 trials) was drawn from the set-size 1 or 2 condition. The remaining compound trials were then used to train a linear SVM classifier to distinguish between activity evoked in set-size 1 and set-size 2 conditions. This classifier was then tested on the trial that was left out of the training procedure. To keep the number of training examples equal between the two conditions, a random selection of trials was removed from the condition with the most trials. The classification was performed repeatedly until each compound trial was used to test the classifier once, thus yielding one classifier outcome per compound trial. These classifier outcomes were averaged to yield a single decoding accuracy score for a given participant and a given timepoint. This procedure was repeated for every timepoint of a trial, and for every participant, and for classifying between each of six possible pairs of set-size condition. In a final step, decoding accuracies from all six classification pairs were averaged (per timepoint) to obtain an overall classification performance for set-size.

Decoding: temporal generalization

To test whether the specific patterns of alpha-band power reflecting the different set-size conditions were stable or dynamic (i.e., varying over time), we performed a temporal generalization decoding approach. The procedure was identical to that of the timepoint-by-timepoint decoding describe above, with the exception that the linear SVM trained at one time point was not only tested on the same time point at which it was trained, but also tested on all

other time points (King & Dehaene, 2014). Thus, the temporal generalization analyses resulted in a 2-dimensional matrix of decoding accuracies, wherein each timepoint in a trial is used for training and for testing the classifier. If the pattern of alpha-band power reflecting specific set-sizes is dynamically changing over time, significant decoding should be found only along the diagonal line (which is the same data as the timepoint-by-timepoint classification analysis described above). If the alpha oscillation pattern underlying classification performance is stable throughout the delay interval, significant decoding should not only be found along the diagonal line, but also spreading over all combinations of training and testing times during the maintenance period, resulting in a square-like shape of significant decoding performance.

Decoding: statistics

To test for significance in the timepoint-by-timepoint decoding analysis, we followed the same cluster-based permutation approach as described for the lateralized univariate responses above. In this case, cluster-based permutation tests were applied to compare decoding accuracy against chance level (0.5 for binary classification). The cluster-level *t* mass was computed across one dimension (i.e., timepoints within a trial). This permutation test was performed for each of the six set-size comparisons as well as the average of all set-size conditions. For the temporal generalization analysis, the same cluster-based permutation approach was used, except that the cluster-level *t* mass was now computed across two dimensions (i.e., train and test timepoints within a trial).

Decoding: feature contributions

To investigate which electrodes contributed to classifier performance, we extracted the average feature contributions of each electrode at all significant decoding time point, separately for the

encoding and maintenance period. The rationale is that feature contribution is only interpretable when decoding is significantly different from chance. Specifically, in all six pairwise comparisons of set-size, for each participant, for each electrode, and for each (significant) timepoint, we first extracted the absolute feature weight (the length of the support vector, i.e., the vector orthogonal to the hyperplane). These weights were then averaged across significant set-size conditions, and across (significant decoding) timepoints, separately for the encoding and maintenance periods. Finally, the group level feature contribution maps were obtained by averaging the individual feature contribution maps across participants. This resulted in two topographic maps showing each channel's contribution to set-size decoding, during the encoding phase and during the maintenance phase.

To test which electrodes significantly contributed to set-size decoding, we performed a permutation test. On each of 1000 permutations, we randomly shuffled the feature weights across electrodes, and then applied the exact same analysis steps as described above for the observed data. For each electrode, we then computed the proportion of permutations containing any feature contribution at least as high as the feature contribution for that electrode in the observed data. These proportions were interpreted as *p*-values that implicitly account for multiple comparisons (i.e., across electrodes).

3 Results

3.1 Behavioral data

For accuracy, we found decisive evidence ($BF_{incl} = 7.85 \times 10^{26}$) in favor of a main effect of Set-size (Figure 2a). Subsequent pairwise analyses, provided overwhelming evidence that accuracy differed between all set-size conditions (all $BF_{incl} > 2.59 \times 10^{5}$), showing that accuracy dropped dramatically as the set-size increased. This indicates that the manipulation

of auditory WM load was successful. We found no evidence for a main effect of Attended side (BF_{incl} =.73), and substantial evidence against an interaction of Set-size and Attended side (BF_{incl} = .14). Thus, accuracy did not systematically depend on left versus right presentation of the memory array.

For working memory capacity, we also found decisive evidence ($BF_{incl} = 2.68 \times 10^8$) in favor of a main effect of Set-size (Figure 2b). In follow-up analyses, we found evidence that WM capacity was lower in Set-size 1 than in Set-sizes 2, 3, and 4 (all $BF_{incl} > 2.52 \times 10^5$), and that WM capacity was lower in Set-size 2 than in Set-size 3 (BF_{incl} = 76.87). We found no conclusive evidence that WM capacity differed between Set-sizes 2 and 4 (BF_{incl} = 1.47), and we found evidence against a difference in WM capacity between Set-sizes 3 and 4 (BF_{incl} = .15). Finally, we found no conclusive evidence for a main effect of Attended side (BF_{incl} = .41), and we found evidence against an interaction of Set-size and Attended side (BF_{incl} = .09).

Together, these behavioral results demonstrate that estimated WM capacity initially increased as the set-size increased, but then leveled off when set-size (the number of items to be memorized) reached 3, and the corresponding WM capacity *K* equaled about 2 items. The relatively low capacity for auditory WM is largely consistent with previous studies (Alunni-Menichinin et al., 2014; Li et al., 2013; Prosser, 1995), in which researchers also found the maximum capacity of auditory WM was 2.8, 2.9 and 2 pure tones, respectively. Importantly, this plateau establishes that the ceiling of auditory WM capacity (in the present experimental setting) is somewhere between two to three pitches of pure tones, and indicates that our higher set-size condition(s) exceeded capacity limitations.

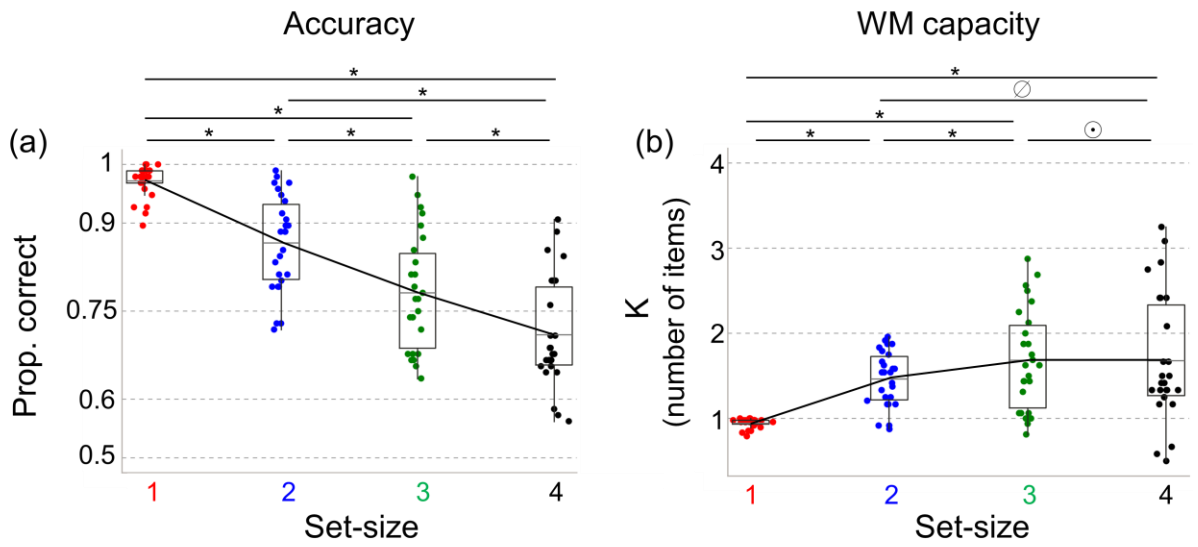

Figure 2. Results of behavioral performance. Panel (a) shows the accuracy, and panel (b) shows the auditory working memory capacity estimate *K,* separately for set-size 1 (red), 2 (blue), 3 (green) and 4 (black) conditions. In all plots, the mid-black-line in the box plot represents the group mean. * indicates evidence in favor of the post-hoc differences; ø indicates inconclusive evidence ($1/3 < BF_{10} < 3$); ⊙ indicates evidence against the post-hoc difference.

3.2 Lateralized univariate responses

To test whether auditory working memory load was reflected in lateralized neural responses, akin to the CDA for visual WM load, we calculated interhemispheric difference for each set-size condition for both mean univariate responses (time domain) and mean alpha-band power (frequency domain) during the maintenance interval. Two cluster-based permutation tests were performed to test (1) whether an overall lateralized response is observed during the maintenance period, reflecting the side of the attended memory items, and (2) whether this putative lateralized response scales with set-size.

Testing for a lateralized response across set-sizes in the time domain revealed a significant cluster across the whole maintenance period (between 1400 and 3400 ms after

stimulus onset), with stronger contralateral compared to unilateral activity (*t*-mass $= -2.53 \times 10^3$, $p < .001$). This negative cluster was most pronounced at the temporal electrodes. This negative difference waves confirms the existence of a CDA-like response during the maintenance interval, indicating the validity of our attention manipulation (Figure 3a). This lateralized response, however, did not differ between set-size conditions (no significant clusters were observed), suggesting that auditory WM load is not reflected in lateralized responses.

Conducting the same two analyses with alpha-band power (in the frequency domain) revealed no significant clusters (Figure 3b); neither when collapsing across set-sizes, nor when testing for differences between set-sizes.

In sum, substantial lateralized responses were found in the time domain, reflecting which side was attended for the memory task. This demonstrates that our attention manipulation (attend left or attend right) was successful. However, we found no evidence that auditory WM load was reflected in lateralized responses, neither in the time nor in the frequency domain, suggesting that the CDA is a modality-specific rather than supra-modal marker for visual WM load only.

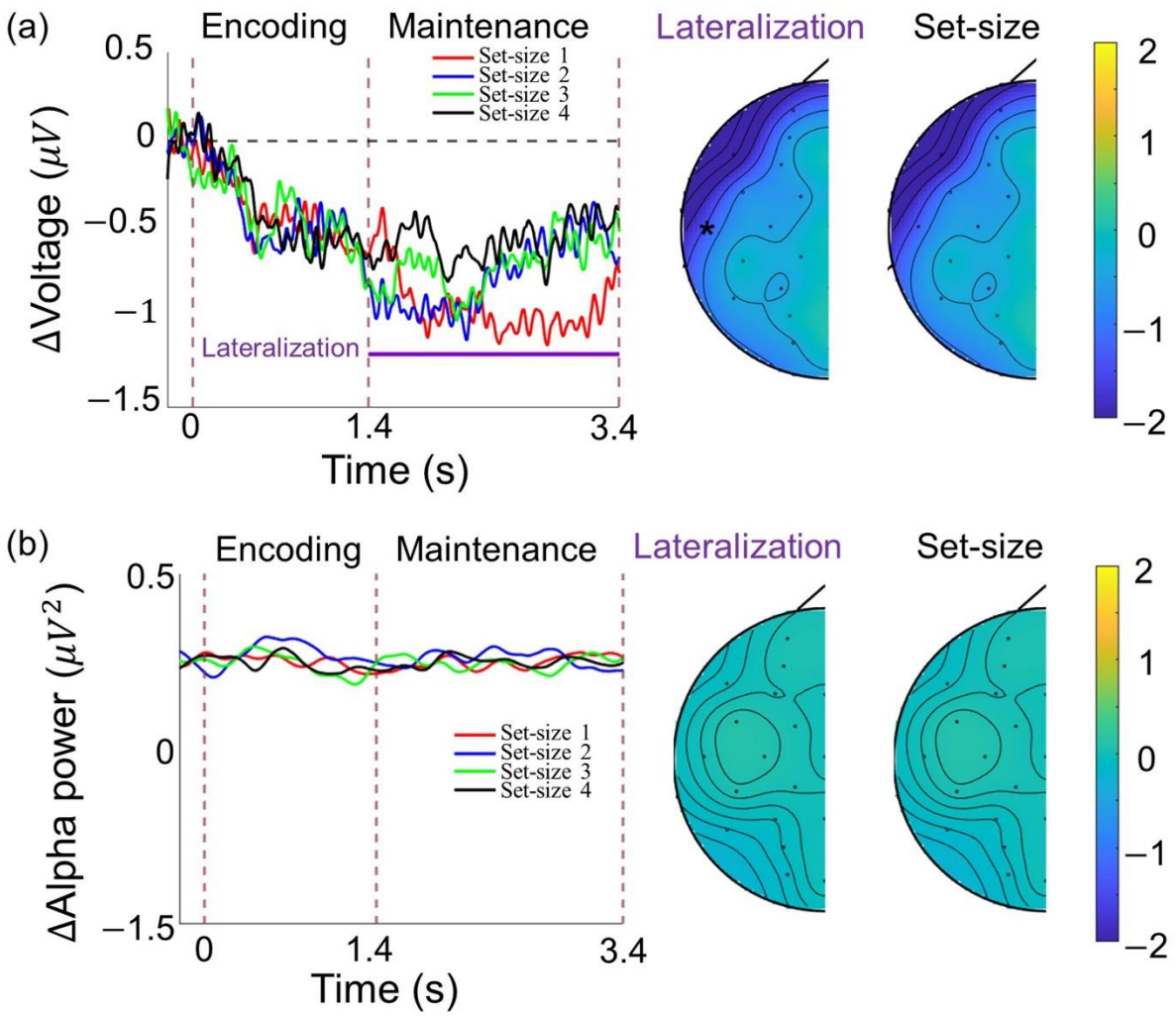

551

552 **Figure 3.** Lateralized (contralateral minus ipsilateral) response, and its topographical distribution. (a) Left:
553 Lateralized response in the time domain data measured in the Set-size 1 (red), 2 (blue), 3 (green), and 4 (black)
554 conditions. The vertical dashed lines indicate (from left to right) the onset of the tone sequence, the onset of the
555 maintenance period, and the end of the maintenance period. The horizontal purple line indicates a significant
556 lateralized effect (deviating from 0) collapsed across all four set-size conditions. Below that, the absence of a line,
557 indicates that this lateralized response was not modulated by set-size. Right: The two topographical maps depict
558 (1) the magnitude of the lateralized response averaged across four set-size conditions during the time window
559 with significant lateralized effects and (2) the extent to which this response differs between set-size conditions,
560 during the maintenance period. Electrodes where these effects are significant are marked with an * (if any) . Panel
561 (b) depicts the same as Panel (a), but for lateralized alpha-band power.

562

3.3 Alpha-band power decoding

Timepoint-by-timepoint classification

We set out to test whether WM load could be decoded from scalp patterns of EEG alpha-band oscillations. To this end, we trained a linear SVM classifier to distinguish between patterns of alpha-band power evoked by different set-size conditions. For this first decoding analysis, the classifier was trained and tested using data from the same time point in a trial (i.e., timepoint-by-timepoint decoding), ranging from the onset of the memory sequence to the end of maintenance period. The results of the cluster-based permutation test showed that, overall, set-size could be reliably decoded from alpha-band power from around 450 ms after the onset of the memory sequence, until around 3000 ms, thereby covering most of the encoding and maintenance period (1 cluster, $p < .001$; see Figure 4). The analysis of feature contributions showed that decoding of set-size – in both the encoding and maintenance period – was largely driven by bilateral temporal electrodes. Thus, auditory WM load can be decoded from (mostly temporal) scalp patterns of alpha-band power.

We then investigated for each pair of set-size conditions individually, whether they evoked discriminable scalp patterns of alpha-band power (i.e., 1 vs 2, 1 vs 3, 1 vs 4, 2 vs 3, 2 vs 4, and 3 vs 4). As can be seen in the six smaller panels of Figure 4, significant decoding during the maintenance period was found for the set-size 1 versus 2 (1300 ms to 1750 ms; 1 cluster, $p < .001$), set-size 1 versus 3 (1400 ms to 2200 ms, and 2300 ms to 3000 ms; 2 clusters, both $p < .01$), and set-size 1 versus 4 (1400 ms to 2650 ms, and 2850 ms to 3050 ms; 2 clusters, both $p < .05$). These results that patterns of alpha-band oscillations during the maintenance period distinguish between set-sizes of 1 and higher, but do not allow to distinguish between set-sizes of 2 and higher (which are above the group-level capacity estimations).

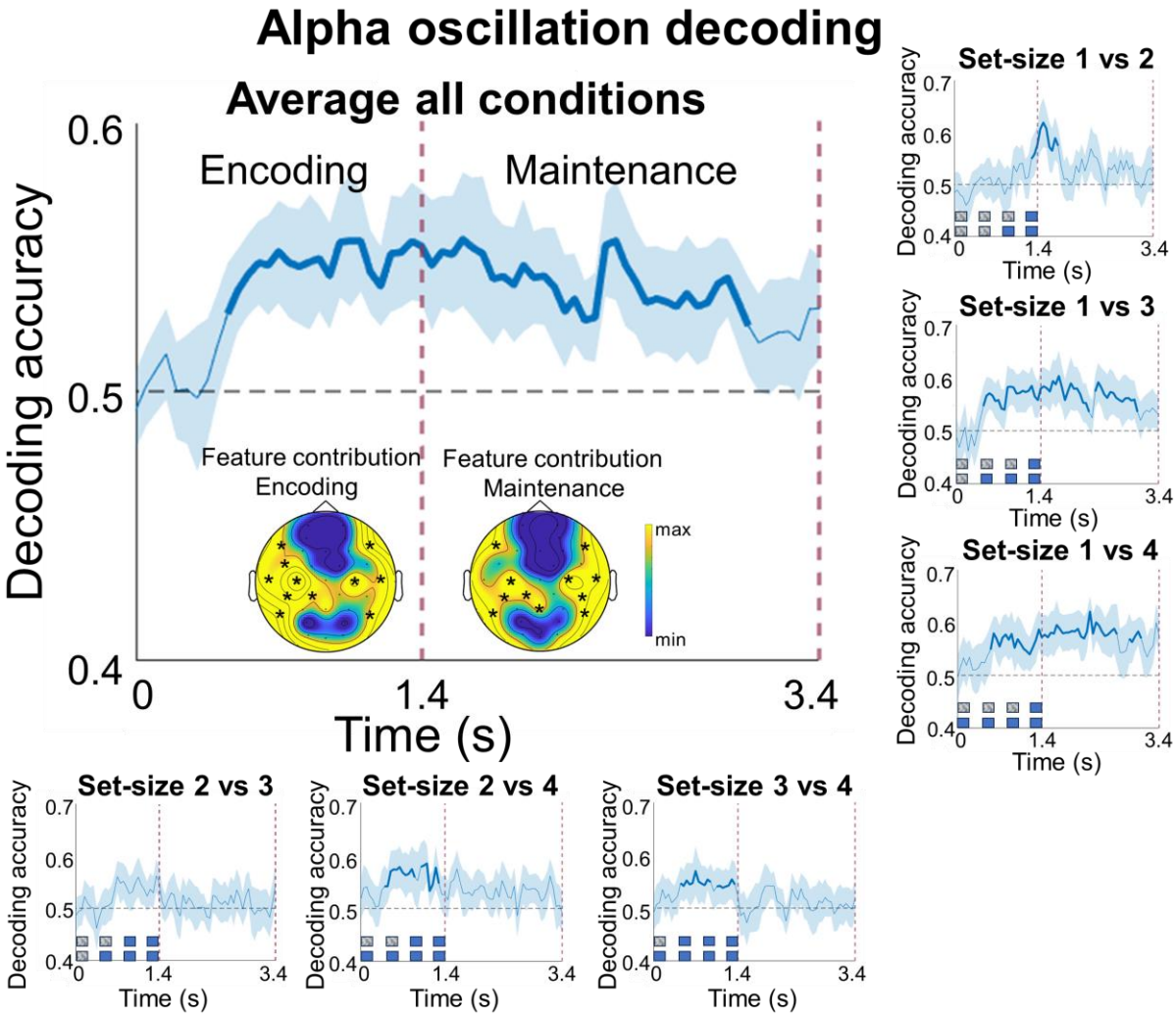

587

588 **Figure 4.** Timepoint-by-timepoint decoding of scalp patterns of alpha-band (8-12 Hz) power. All panels depict
589 decoding accuracy (y-axis) as a function of time (x-axis). The big panel depicts decoding accuracy averaged across
590 all six pairwise comparisons (i.e., main effect set-size), which are depicted individually in the surrounding smaller
591 panels. Bold blue lines indicate significant above chance (50%) decoding, based on cluster-based permutation
592 testing to account for multiple comparisons. The vertical dashed-purple lines split time into the encoding and
593 maintenance periods. The two topographical maps depict the extent to which each electrode contributed to
594 decoding performance, separately for the encoding and maintenance period. Electrodes with significant feature
595 contribution are marked with an *. In the small panels, the blue squares indicate the target tones, while the blurred
596 squares indicate the white noise.

597

598 *Temporal generalization*

In a final set of analyses, we set out to test whether the scalp patterns of alpha-band power reflecting auditory WM load are stable, or vary dynamically over the course of the maintenance period. To this end, we performed temporal generalization analyses, whereby linear SVM classifiers were trained and tested on data from all possible combinations of timepoints (thus yielding a 2D decoding matrix, instead of a time-series). When considering all set-sizes together, we replicated the finding that set-size can be decoded from scalp patterns of alpha-band power during the maintenance period (from 400 ms to 3400 ms, 1 cluster, $p < .001$). Importantly, the present analysis also shows that significant set-size decoding (depicted in black in Figure 5) is way more prevalent on-diagonal than off-diagonal, indicating that the specific pattern of alpha-band power associated with different set-sizes varies over the course of the maintenance period.

These findings are largely confirmed when considering the six set-size comparisons in isolation. As shown in the six smaller panels, temporal generalization decoding revealed significant decoding for set-sizes 1 versus 2 (1300 ms to 1850 ms; 1700 ms to 3250 ms, 2 clusters, both $p < .05$), 1 versus 3 (400 ms to 3250 ms, 1 cluster, $p < .001$), and set-size 1 versus 4 (0 ms to 3400 ms, 1 cluster, $p < .001$). Again, no significant decoding performance was found for set-sizes 2 versus 3, 2 versus 4, and 3 versus 4, thus mirroring the results of the timepoint-by-timepoint decoding analysis.

In sum, we found that scalp patterns of alpha-band power during the maintenance period reflects auditory WM load, with bilateral temporal electrodes contributing most to decoding performance. These load-specific EEG responses allowed to distinguish between load conditions up to the group-level capacity limitations, but not between load conditions exceeding this limit, as established from the behavioral data (i.e., around K = 2). Interestingly, the specific patterns of alpha-band power that reflected specific set-size conditions evolved dynamically across the maintenance period, suggesting the dynamic coding of auditory WM

load.

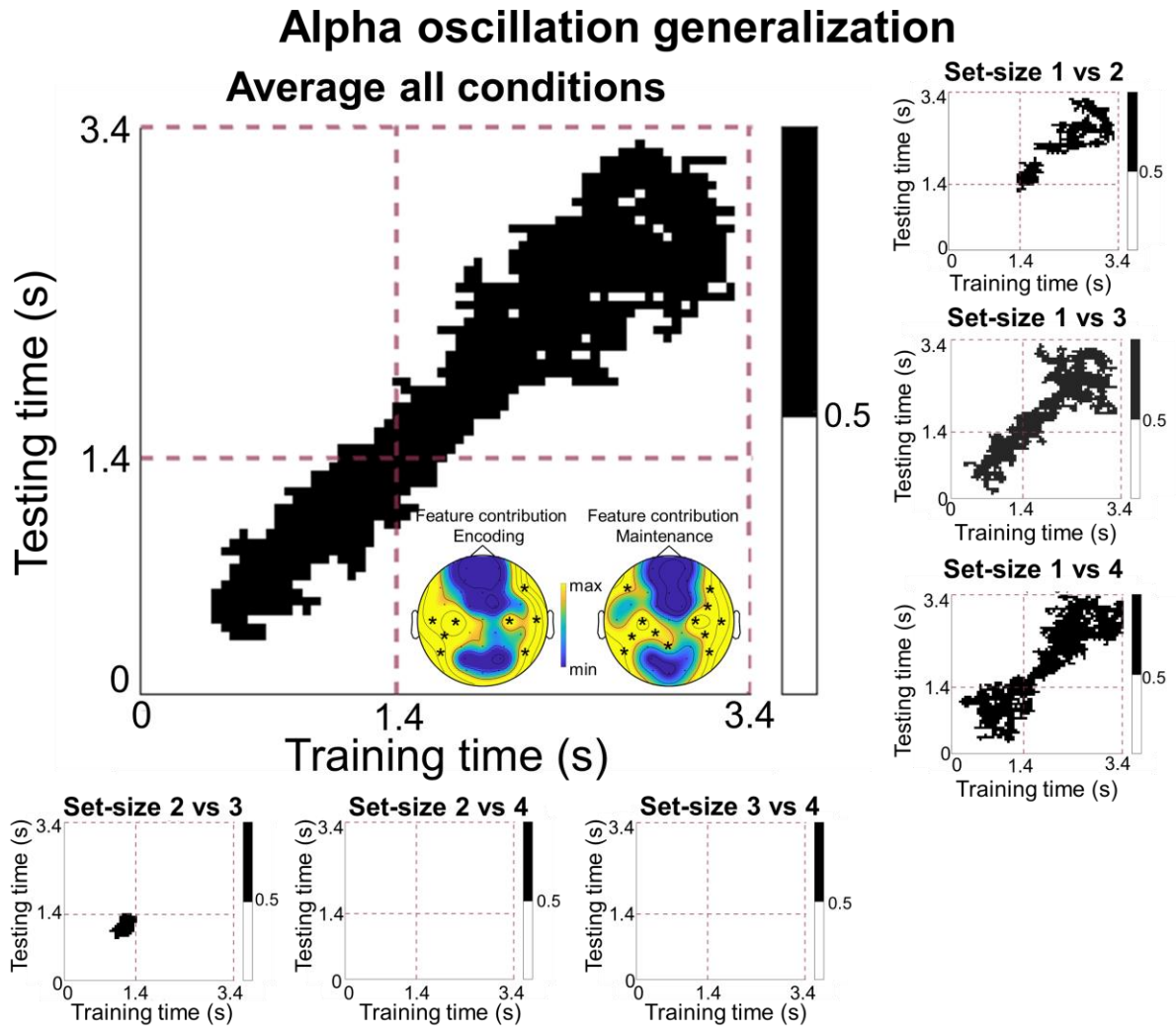

Figure 5. Temporal generalization decoding of scalp patterns of alpha-band (8-12 Hz) power. The big panel depicts decoding accuracy averaged across all six pairwise comparisons (i.e., main effect set-size), which are depicted individually in the surrounding smaller panels. In each plot, each data point corresponds to a classification analysis performed with training data from one time point (x-axis) and tested on another time point (y-axis). Black data points in each plot indicate significant above chance (50%) decoding, based on cluster-based permutation testing to account for multiple comparisons. The dashed-purple lines split time into encoding and maintenance periods. The two topographical maps depict the extent to which each electrode contributed to decoding performance, separately for the encoding and maintenance period. Electrodes with significant feature contribution are marked with an *.

4 General Discussion

In the present study, we set out to investigate whether auditory WM load is reflected in lateralized neural responses, akin to the CDA for visual WM load. We further attempted to identify other (non-lateralized) load-dependent neuro-markers of auditory WM, using multivariate pattern analysis (MVPA). To these aims, we recorded EEG while participants were holding the pitches of 1, 2, 3, or 4 tones in WM for a subsequent auditory recognition task. The behavioral results showed that auditory WM capacity plateaued between two and three tones. Two key findings emerged from the analyses of EEG data. First, although we identified a lateralized (CDA-like) response during the maintenance period, this response did not scale with set-size; neither in the time nor in the frequency (alpha oscillation) domain. Thus, we found no evidence that WM load was reflected in lateralized responses. Second, using MVPA, we found that scalp patterns of alpha-band power during the maintenance period reflected auditory WM load. These load-specific EEG responses were mostly confined to bilateral temporal channels, and allowed to distinguish between set-size conditions up until –but not above– group level capacity limitations (i.e., about 2 items, based on the behavioral data). Interestingly, we also found that the scalp patterns of alpha-band power reflecting specific auditory WM were not stable across the maintenance period. Instead, these patterns dynamically changed across the maintenance period, with patterns evoked at the start of the maintenance period barely generalizing to patterns at the end of the interval, and vice versa. In short, our results show that dynamic scalp patterns of alpha-band power can be used as a novel neuro-marker of auditory WM load. In the following sections, we will first discuss what it means that (unlike for visual WM load) auditory WM load is not reflected in lateralized responses. Then, we will elaborate on the scalp patterns of alpha power that were shown to track auditory WM load, and discuss what they tell us about the neural coding of auditory WM.

4.1 No lateralized responses to auditory WM load

In the current study, we identified a lateralized univariate response during the WM delay, akin to the CDA for visual WM. Unlike the CDA, however, we found no evidence that the lateralized response to auditory WM was modulated by load, neither in the time nor in the frequency domain. That is, where the amplitude of the CDA increases when visual WM load increases, the lateralized responses to auditory WM load observed in our study did not differ between load conditions. This raises the question why auditory WM load is not reflected in lateralized responses, while visual WM load is, even when both require the maintenance of lateralized sensory input? We approach this question from a cognitive, an anatomical, and a functional perspective.

From a cognitive perspective, our results can be framed in the context of the multi-component model of WM, proposed by Baddeley and Hitch (1974). The absence of a lateralized response to auditory WM load entails that the CDA of visual WM reflects load in the visuo-spatial sketchpad specifically, and does not reflect load in the domain-general central executive or episodic buffer. Thus, although regulating the quantity of information in WM (i.e., load) may be regarded as an executive process, sustained neural responses tracking visual WM load (i.e., the CDA) may instead be more sensory-like, and depend on the specific content that is maintained in WM. This may explain why neural markers of WM load are not so much observed in frontal electrodes – that are typically associated with executive processes – but tend to arise in sensory-specific processing regions. That is, the CDA is typically most pronounced in posterior electrodes for visual WM, and we found neural responses tracking auditory WM load (scalp patterns of alpha power, discussed below) to arise predominantly around temporal electrodes. Accordingly, different modalities may rely on qualitatively distinct storage mechanisms.

From an anatomical perspective, the differences between visual and auditory WM may

be due to the difference in the visual and auditory processing pathways, leading from sensory receptors to the cortex. For the visual pathway, due to the optic chiasm, items presented in the left hemifield are projected to the right primary visual cortex, whereas items presented to the right hemifield are projected to the left primary visual cortex (De Moraes, 2013; Rodieck, 1979). Thus, these hemisphere specific responses during stimulus encoding may foster a difference between contralateral and ipsilateral responses during the WM delay, when items on one side are to be remembered while items on the other side are to be ignored. In the case of auditory processing, however, the input to each ear is first extensively processed and combined subcortically, before being projected to the left and right primary auditory cortex (Pickles, 2015). Specifically, the superior olivary complex receives information from both contralateral and ipsilateral ears, to support sound localization. Then the auditory information is projected to both contralateral and ipsilateral sides of the superior colliculus (Hackney, 1987), before projecting to the primary auditory cortices. Thus, for the auditory pathway, tones presented via the left or right ear activate both the left and right auditory cortex, albeit with a bias toward the contralateral auditory cortex (Lipschutz et al., 2002; Woldorff et al., 1999). This slight contralateral dominance in auditory processing might explain the overall lateralized responses that we observed during the WM delay. Importantly, however, contralateral dominance is much weaker in auditory processing than in visual processing, because auditory input from both ears is largely integrated sub-cortically (Schwartz, 1992). This reduced lateralization during auditory processing may explain the absence of a load-dependent modulation in lateralized responses for auditory WM load.

From a functional perspective, the reason for why we did not find a lateralized response to auditory WM load might stem from the different organizational principles of auditory compared to visual information. In visual WM tasks, visual information is processed via spatial coding, while in the auditory WM task, auditory information may be processed through

711 temporal coding. For instance, recent evidence has shown that observers use spatial location as
712 an organizational principle to help maintain visual information, even if the spatial location is
713 irrelevant for the task at hand (Arora et al., 2024; van Ede et al., 2019). In contrast, several
714 studies have shown that auditory spatial information only has an effect on alpha lateralization
715 in working memory and perception task when space is relevant for the task at hand (Klatt et al.,
716 2018a; Klatt et al., 2018b). In the current study, the spatial location was irrelevant for the
717 auditory WM recognition task, because the location was always the same for all memorized
718 items in a block. Moreover, sustained attention to same location (due to our block design) may
719 reduce the strength of lateralized responses, as previous studies have shown increases in alpha
720 lateralization after the sound source changes location (Getzmann et al., 2020). In contrast to
721 the spatial organization observed during the maintenance of visual WM items, the maintenance
722 of auditory WM items (such as pitches of pure tones) may be organized within a temporal
723 reference frame, by iterating through the different items over time. This interpretation fits well
724 with the classical example of the phonological loop (the auditory counterpart of the visuo-
725 spatial sketchpad) as the repetition of sequences of items over time, such as the digits of a to-
726 be-memorized phone number. If auditory WM items are indeed segregated over time, a
727 lateralized (univariate) neural response to load is not expected to differ at any given timepoint
728 (in a singular brain area), because the load within each timepoint is always 1. The finding that
729 our neural markers of auditory WM load appear to change over the course of the maintenance
730 period (see below), is very much in line with this idea of temporal coding.

731

732 4.2 Alpha patterns reflecting auditory WM load

733 Using both timepoint-by-timepoint decoding and temporal generalization decoding, we
734 found that scalp patterns of alpha-band power during the delay period allowed to distinguish
735 between individual load conditions up until WM capacity limitations (Set-size 1 vs 2, 1 vs 3, 1

vs 4). In contrast, patterns of alpha-band power during maintenance could not distinguish between load conditions that exceeded capacity limitations based on the behavioral results (Set-size 2 vs 3, 2 vs 4, 3 vs 4). The correspondence between these behavioral results and decoding results further substantiates that patterns of alpha-band power specifically reflect auditory WM load. The differences in alpha-band power between load conditions might reflect differences in executive demands, which scale with the number of tones held in working memory (Leiberg et al., 2006). The more tones held in memory, the more resources had to be allocated over areas where representations of the to-be-memorized stimuli are presumably stored. Previous studies have also found that alpha oscillations are involved in auditory WM. In these studies, the role of alpha oscillations is interpreted to reflect top-down inhibition of task-irrelevant sensory input and/or task-irrelevant neural processes (Kaiser et al., 2007; Van Dijk et al., 2010; Wilsch & Obleser, 2016). Most of the studies, however, compared responses in a memory task to that of a non-memory control task, and found stronger alpha-band power in the memory task. Therefore, during the maintenance period in the memory task, participants had to inhibit irrelevant information for successful retention while participants did not need to do so in the non-memory control task. In the current study, we instead compared different load conditions. In these different load conditions, the number of to-be-remembered items (presented to the attended side) varied, but the number of to-be-ignored distractor items (presented to the unattended side) was constant. The set-size of the distractors, therefore, did not covary with the set-size of the memory items. As such, the differences in scalp patterns of alpha-band power between set-size conditions reflect WM load, rather than distractor inhibition. Thus, our findings reveal the role of alpha oscillations in the maintenance of information in auditory WM.

The absence of generalization between the encoding and maintenance period (in our temporal generalization analyses) indicates that our significant decoding during the maintenance period specifically reflect maintenance-related process, rather than residual

761 signals from the encoding period. Focusing on the maintenance period, our temporal
762 generalization analyses suggest that the scalp patterns of alpha-band power associated with
763 specific WM loads are not stable over time, but change over the course of the maintenance
764 period. One possible interpretation of this, is that auditory WM load is inherently represented
765 through dynamic coding (akin to visual WM content; see Stokes, 2015). In the context of load,
766 changing neural representations may also reflect the interplay, over time, between sensory
767 regions involved in maintenance, and frontal regions involved in executive processes. Another,
768 potentially related possibility, could be that participants were maintaining the different pitches
769 sequentially (i.e., as they were presented). In this scenario, the changing patterns of alpha-band
770 power associated with specific load conditions, may reflect the duration of the sequence or the
771 number of consecutive items in a sequence. It should be noted, though, that in the later stages
772 of the delay period, we did observe some off-diagonal decoding, indicating some temporal
773 generalization of the load-specific responses. This may either reflect smearing out of the load-
774 specific responses as they desynchronize over time, or it may reflect the stabilization of the
775 memory content into a format that is relevant for the upcoming test (the timing of which was
776 predictable). During most of the delay period, however, decoding of individual load conditions
777 was substantially more pronounced on the diagonal compared to the off-diagonal. We therefore
778 conclude that, overall, patterns of alpha-band power reflecting auditory WM load change
779 dynamically during the maintenance period. Future research is needed to understand what
780 cognitive processes or storage mechanisms underly these dynamics.

781 If neural markers of WM load (such as scalp patterns of alpha-band power) are modality
782 specific, they would be expected to mostly involve sensory processing regions. Indeed, we
783 found that bilateral temporal electrodes (roughly corresponding to primary auditory cortices)
784 contributed the most to the decoding of auditory WM load, and this was consistent between the
785 encoding and maintenance periods. This finding is in line with the involvement of bilateral

786 temporal regions for the encoding and maintaining of different quantities of tones. Previous
787 studies have shown the involvement of temporal regions, including auditory cortex, in auditory
788 WM (Gaab et al., 2003; Grimault et al., 2014; Koelsch et al., 2009). Importantly, here we show
789 that patterns of alpha-band power in these temporal electrodes scale with set-size, and can
790 therefore be used to distinguish between auditory WM load conditions. Furthermore, the fact
791 that the feature contribution maps was similar in the encoding and maintenance period suggests
792 that the maintenance of sequences of sound pitches might recruit the same neural circuits that
793 are involved in the sensory encoding of these same sound pitches. This is in line with the
794 sensory recruitment hypothesis (Gayet et al., 2018; Katus et al., 2015; Scimeca et al., 2018;
795 Silvanto & Soto, 2012), which has been more extensively studied in visual WM, and proposes
796 that the same neural populations that represent sensory features during perception are also
797 recruited during WM maintenance, thereby reducing cortical redundancy. On the other hand,
798 the results of our temporal generalization analyses show that, despite the overlap in brain
799 regions underlying load during encoding and maintenance, the activity patterns underlying the
800 different load conditions did not generalize between the encoding and maintenance periods.
801 This suggests that perceptual load (encoding) and WM load (maintenance) are reflected in
802 shared neural populations, within domain-specific brain regions.

803

804 4.3 Limitations

805 One may argue that the capacity of auditory WM is relative low (around 2 tones) in the current
806 study. However, this relatively low capacity is largely consistent with previous studies (Alunni-
807 Menichinin et al., 2014; Li et al., 2013; Prosser, 1995), in which researchers also found the
808 maximum capacity of auditory WM was 2.8, 2.9 and 2 pure tones, respectively. It should be
809 noted that calculations of WM capacity are estimates, and do not reflect perfect measurement
810 of WM capacity. Indeed, capacity estimates should theoretically remain constant across set-

size conditions, but the estimate of WM capacity K, is known to vary when large differences in set-size are used (Rouder et al., 2011). Thus, it is unclear whether auditory WM capacity in our study should be estimated to be around 2 items (the actual capacity estimate K) or at ~3-4 items (the set-size conditions at which the capacity estimate K started to plateau). Could the challenging dichotic presentation tasks employed in our have reduced capacity estimates? Studies using binaural stimulation typically show that observers can ignore the unattended auditory stream with little to no effort, yielding virtually no interference to the processing of the attended auditory stream (Alho et al., 1994; Carpenter et al., 2002). Thus, the use of binaural stimulation is unlikely to have substantially reduced capacity estimations in our study. Taken together, the present behavioral results cannot be taken to reflect a universal auditory WM capacity limit, but they do demonstrate the relatively low capacity as compared to (for instance) visual WM in similar task designs. [1]

4.4 Conclusion

In conclusion, we observed two main findings in the current study. First, we found no evidence that auditory WM load is reflected in lateralized responses – neither in the time nor in the frequency domain. This implies that CDA-like responses as observed for visual WM load are vision-specific rather than domain general markers of WM load. The lack of location-specific response further suggests that auditory WM is not inherently spatially organized, as is the case for visual WM. Second, using multivariate pattern analyses, we found that (mostly temporal) scalp patterns of alpha-band power during the maintenance period reflect auditory WM load. Interestingly, patterns of alpha-band power reflecting specific load conditions were changing dynamically over the course of the maintenance period, revealing that (1) principles of dynamic

[1] Unlike tasks where verbal labeling is possible, which can greatly increase WM capacity, participants in the present study could not rely on such a strategy. This may have contributed to the observed relatively low capacity estimates.

834 neural population coding –which is known to underly the storage of WM content– may also be
835 extended to executive WM processes, and (2) auditory WM may be inherently temporally
836 organized, reflecting the repetition of information streams over time.

837

838 **Data availability statement**

839 All data, codes to run the experiments, analyze and visualize the data are uploaded to the OSF
840 platform (https://osf.io/mw5ve/).

841

842 **Ethics statement**

843 The study protocols were approved by the faculty ethics committee (FETC) of Utrecht
844 University (number 18-048 van der Stoep). All participants signed informed consent for their
845 participation.

846

847 **Author Contribution**

848 Yichen Yuan: conceptualization, data curation, formal analysis, funding acquisition,
849 methodology, resources, software, validation, visualization, writing—original draft, writing—
850 review and editing. Surya Gayet: conceptualization, methodology, project administration,
851 resources, supervision, writing—original draft, writing—review and editing. Derk Wisman:
852 conceptualization, data curation, investigation, methodology, resources, software, writing—
853 review and editing. Stefan van der Stigchel: conceptualization, methodology, project
854 administration, resources, supervision, writing—review and editing. Nathan van der Stoep:
855 conceptualization, methodology, project administration, resources, supervision, writing—

original draft, writing—review and editing. All authors contributed to the article and approved the submitted version.

Funding

This work was supported by the China Scholarship Council (grant number 202206380011 to Yichen Yuan).

References

Ahissar, M., Lubin, Y., Putter-Katz, H., & Banai, K. (2006). Dyslexia and the failure to form a perceptual anchor. *Nature Neuroscience*, *9*(12), 1558–1564. https://doi.org/10.1038/nn1800

Alho, K., Teder, W., Lavikainen, J., & Näätänen, R. (1994). Strongly focused attention and auditory event-related potentials. *Biological Psychology*, *38*(1), 73–90. https://doi.org/10.1016/0301-0511(94)90050-7

Alunni-Menichini, K., Guimond, S., Bermudez, P., Nolden, S., Lefebvre, C., & Jolicoeur, P. (2014). Saturation of auditory short-term memory causes a plateau in the sustained anterior negativity event-related potential. *Brain Research*, *1592*, 55–64. https://doi.org/10.1016/j.brainres.2014.09.047

Arora, K., Gayet, S., Kenemans, J. L., Van der Stigchel, S., & Chota, S. (2024). Dissociating External and Internal Attentional Selection. *BioRxiv*, 2024-08.

Baddeley A. (2000). The episodic buffer: a new component of working memory?. *Trends in Cognitive Sciences*, *4*(11), 417–423. https://doi.org/10.1016/s1364-6613(00)01538-2

878 Baddeley, A. D., & Hitch, G. J. (1974). Working memory. In G. H. Bower (Ed.), *Psychology of*
879 *Learning and Motivation Vol. 8* (pp. 47-89). New York: Academic Press.
880 https://doi.org/10.1016/S0079-7421(08)60452-1

881 Bell, A. J., & Sejnowski, T. J. (1995). An information-maximization approach to blind
882 separation and blind deconvolution. *Neural Computation*, *7*(6), 1129–1159.
883 https://doi.org/10.1162/neco.1995.7.6.1129

884 Bonnefond, M., & Jensen, O. (2012). Alpha oscillations serve to protect working memory
885 maintenance against anticipated distracters. *Current Biology*, *22*(20), 1969–1974.
886 https://doi.org/10.1016/j.cub.2012.08.029

887 Carlisle, N. B., Arita, J. T., Pardo, D., & Woodman, G. F. (2011). Attentional templates in visual
888 working memory. *The Journal of Neuroscience, 31*(25), 9315–9322.
889 https://doi.org/10.1523/JNEUROSCI.1097-11.2011

890 Carpenter, M., Cranford, J. L., Hymel, M. R., De Chicchis, A. R., & Holbert, D. (2002).
891 Electrophysiologic signs of attention versus distraction in a binaural listening
892 task. *Journal of Clinical Neurophysiology*, *19*(1), 55–60.
893 https://doi.org/10.1097/00004691-200201000-00007

894 Chaumon, M., Bishop, D. V., & Busch, N. A. (2015). A practical guide to the selection of
895 independent components of the electroencephalogram for artifact correction. *Journal*
896 *of Neuroscience Methods*, *250*, 47–63. https://doi.org/10.1016/j.jneumeth.2015.02.025

897 Cowan N. (1998). Visual and auditory working memory capacity. *Trends in Cognitive*
898 *Sciences*, *2*(3), 77. https://doi.org/10.1016/s1364-6613(98)01144-9

899 Cowan N. (2010). The Magical Mystery Four: How is Working Memory Capacity Limited,
900 and Why?. *Current Directions in Psychological Science*, *19*(1), 51–57.

https://doi.org/10.1177/0963721409359277

Cowan, N., Elliott, E. M., Scott Saults, J., Morey, C. C., Mattox, S., Hismjatullina, A., & Conway, A. R. (2005). On the capacity of attention: its estimation and its role in working memory and cognitive aptitudes. *Cognitive psychology, 51*(1), 42–100. https://doi.org/10.1016/j.cogpsych.2004.12.001

Czoschke, S., Fischer, C., Bahador, T., Bledowski, C., & Kaiser, J. (2021). Decoding Concurrent Representations of Pitch and Location in Auditory Working Memory. *Journal of Neuroscience*, *41*(21), 4658–4666. https://doi.org/10.1523/JNEUROSCI.2999-20.2021

Delorme, A., & Makeig, S. (2004). EEGLAB: an open source toolbox for analysis of single-trial EEG dynamics including independent component analysis. *Journal of Neuroscience Methods*, *134*(1), 9–21. https://doi.org/10.1016/j.jneumeth.2003.10.009

De Moraes C. G. (2013). Anatomy of the visual pathways. *Journal of Glaucoma*, *22*, S2–S7. https://doi.org/10.1097/IJG.0b013e3182934978

Deutsch D. (1970). Tones and numbers: specificity of interference in immediate memory. *Science*, *168*(3939), 1604–1605. https://doi.org/10.1126/science.168.3939.1604

Diamantopoulou, S., Poom, L., Klaver, P., & Talsma, D. (2011). Visual working memory capacity and stimulus categories: a behavioral and electrophysiological investigation. *Experimental Brain Research, 209*(4), 501–513. https://doi.org/10.1007/s00221-011-2536-z

Faul, F., Erdfelder, E., Buchner, A., & Lang, A. G. (2009). Statistical power analyses using G*Power 3.1: tests for correlation and regression analyses. *Behavior Research*

924 *Methods, 41*(4), 1149–1160. https://doi.org/10.3758/BRM.41.4.1149

925 Gaab, N., Gaser, C., Zaehle, T., Jancke, L., & Schlaug, G. (2003). Functional anatomy of pitch
926 memory--an fMRI study with sparse temporal sampling. *NeuroImage*, *19*(4), 1417–
927 1426. https://doi.org/10.1016/s1053-8119(03)00224-6

928 Gayet, S., Paffen, C. L. E., & Van der Stigchel, S. (2018). Visual Working Memory Storage
929 Recruits Sensory Processing Areas. *Trends in Cognitive Sciences*, *22*(3), 189–190.
930 https://doi.org/10.1016/j.tics.2017.09.011

931 Getzmann, S., Klatt, L. I., Schneider, D., Begau, A., & Wascher, E. (2020). EEG correlates of
932 spatial shifts of attention in a dynamic multi-talker speech perception scenario in
933 younger and older adults. *Hearing Research*, *398*, 108077.
934 https://doi.org/10.1016/j.heares.2020.108077

935 Grimault, S., Nolden, S., Lefebvre, C., Vachon, F., Hyde, K., Peretz, I., Zatorre, R., Robitaille,
936 N., & Jolicoeur, P. (2014). Brain activity is related to individual differences in the
937 number of items stored in auditory short-term memory for pitch: evidence from
938 magnetoencephalography. *NeuroImage*, *94*, 96–106.
939 https://doi.org/10.1016/j.neuroimage.2014.03.020

940 Hackney C. M. (1987). Anatomical features of the auditory pathway from cochlea to cortex.
941 *British Medical Bulletin, 43*(4), 780–801.
942 https://doi.org/10.1093/oxfordjournals.bmb.a072218

943 Harrison, S. A., & Tong, F. (2009). Decoding reveals the contents of visual working memory
944 in early visual areas. *Nature*, *458*(7238), 632–635. https://doi.org/10.1038/nature07832

945 Hugdahl K. (2011). Fifty years of dichotic listening research - still going and going
946 and…. *Brain and Cognition*, *76*(2), 211–213.

https://doi.org/10.1016/j.bandc.2011.03.006

JASP Team (2024). JASP (Version 0.19.0)[Computer software].

Jensen, O., Gelfand, J., Kounios, J., & Lisman, J. E. (2002). Oscillations in the alpha band (9–12 Hz) increase with memory load during retention in a short-term memory task. *Cerebral Cortex*, *12*(8), 877–882. https://doi.org/10.1093/cercor/12.8.877

Kaiser, J., Heidegger, T., Wibral, M., Altmann, C. F., & Lutzenberger, W. (2007). Alpha synchronization during auditory spatial short-term memory. *Neuroreport*, *18*(11),1129–1132. https://doi.org/10.1097/WNR.0b013e32821c553b

Kass, R. E., & Raftery, A. E. (1995). Bayes factors. *Journal of the American Statistical Association*, *90*(430), 773-795. https://doi.org/10.1080/01621459.1995.10476572

Katus, T., Müller, M. M., & Eimer, M. (2015). Sustained maintenance of somatotopic information in brain regions recruited by tactile working memory. *The Journal of Neuroscience*, *35*(4), 1390–1395. https://doi.org/10.1523/JNEUROSCI.3535-14.2015

Kikumoto, A., & Mayr, U. (2018). Decoding hierarchical control of sequential behavior in oscillatory EEG activity. *eLife*, *7*, e38550. https://doi.org/10.7554/eLife.38550

King, J. R., & Dehaene, S. (2014). Characterizing the dynamics of mental representations: the temporal generalization method. *Trends in Cognitive Sciences*, *18*(4), 203–210. https://doi.org/10.1016/j.tics.2014.01.002

Klatt, L. I., Getzmann, S., Wascher, E., & Schneider, D. (2018a). Searching for auditory targets in external space and in working memory: Electrophysiological mechanisms underlying perceptual and retroactive spatial attention. *Behavioural Brain Research*, *353*, 98–107. https://doi.org/10.1016/j.bbr.2018.06.022

Klatt, L. I., Getzmann, S., Wascher, E., & Schneider, D. (2018b). The contribution of selective

spatial attention to sound detection and sound localization: Evidence from event-related potentials and lateralized alpha oscillations. *Biological Psychology*, *138*, 133–145. https://doi.org/10.1016/j.biopsycho.2018.08.019

Koelsch, S., Schulze, K., Sammler, D., Fritz, T., Müller, K., & Gruber, O. (2009). Functional architecture of verbal and tonal working memory: an FMRI study. *Human Brain Mapping*, *30*(3), 859–873. https://doi.org/10.1002/hbm.20550

Kumar, S., Joseph, S., Gander, P. E., Barascud, N., Halpern, A. R., & Griffiths, T. D. (2016). A Brain System for Auditory Working Memory. *Journal of Neuroscience*, *36*(16), 4492–4505. https://doi.org/10.1523/JNEUROSCI.4341-14.2016

Lefebvre, C., Vachon, F., Grimault, S., Thibault, J., Guimond, S., Peretz, I., Zatorre, R. J., & Jolicoeur, P. (2013). Distinct electrophysiological indices of maintenance in auditory and visual short-term memory. *Neuropsychologia*, *51*(13), 2939–2952. https://doi.org/10.1016/j.neuropsychologia.2013.08.003

Leiberg, S., Lutzenberger, W., & Kaiser, J. (2006). Effects of memory load on cortical oscillatory activity during auditory pattern working memory. *Brain Research*, *1120*(1), 131–140. https://doi.org/10.1016/j.brainres.2006.08.066

Li, D., Cowan, N., & Saults, J. S. (2013). Estimating working memory capacity for lists of nonverbal sounds. *Attention, Perception & Psychophysics*, *75*(1), 145–160. https://doi.org/10.3758/s13414-012-0383-z

Li, Q., & Saiki, J. (2015). Different effects of color-based and location-based selection on visual working memory. *Attention, Perception & Psychophysics*, *77*(2), 450–463. https://doi.org/10.3758/s13414-014-0775-3

Linke, A. C., Vicente-Grabovetsky, A., & Cusack, R. (2011). Stimulus-specific suppression

993 preserves information in auditory short-term memory. *Proceedings of the National*
994 *Academy of Sciences of the United States of America*, *108*(31), 12961–12966.
995 https://doi.org/10.1073/pnas.1102118108

996 Lipschutz, B., Kolinsky, R., Damhaut, P., Wikler, D., & Goldman, S. (2002). Attention-
997 dependent changes of activation and connectivity in dichotic listening. *NeuroImage,*
998 *17*(2), 643–656. https://doi.org/10.1006/nimg.2002.1184

999 Luck, S. J., & Vogel, E. K. (1997). The capacity of visual working memory for features and
1000 conjunctions. *Nature*, *390*(6657), 279–281. https://doi.org/10.1038/36846

1001 Luo, H., Husain, F. T., Horwitz, B., & Poeppel, D. (2005). Discrimination and categorization
1002 of speech and non-speech sounds in an MEG delayed-match-to-sample
1003 study. *NeuroImage*, *28*(1), 59–71. https://doi.org/10.1016/j.neuroimage.2005.05.040

1004 Luria, R., & Vogel, E. K. (2011). Shape and color conjunction stimuli are represented as bound
1005 objects in visual working memory. *Neuropsychologia*, *49*(6), 1632–1639.
1006 https://doi.org/10.1016/j.neuropsychologia.2010.11.031

1007 Maris, E., & Oostenveld, R. (2007). Nonparametric statistical testing of EEG- and MEG-
1008 data. *Journal of Neuroscience Methods*, *164*(1), 177–190.
1009 https://doi.org/10.1016/j.jneumeth.2007.03.024

1010 Mathôt, S. (2017). Bayes like a Baws: Interpreting Bayesian repeated measures in
1011 JASP. *Cognitive Science and more*, *6*, 66. https://www.cogsci.nl/blog/interpreting-
1012 bayesian-repeated-measures-in-jasp

1013 Oostenveld, R., Fries, P., Maris, E., & Schoffelen, J. M. (2011). FieldTrip: Open source
1014 software for advanced analysis of MEG, EEG, and invasive electrophysiological

1015 data. *Computational Intelligence and Neuroscience*, *2011*, 156869.
1016 https://doi.org/10.1155/2011/156869

1017 Peelen, M. V., & Downing, P. E. (2023). Testing cognitive theories with multivariate pattern
1018 analysis of neuroimaging data. Nature Human Behaviour, 7(9), 1430–1441.
1019 https://doi.org/10.1038/s41562-023-01680-z

1020 Pickles J. O. (2015). Auditory pathways: anatomy and physiology. *Handbook of Clinical*
1021 *Neurology*, *129*, 3–25. https://doi.org/10.1016/B978-0-444-62630-1.00001-9

1022 Pratt, H., Michalewski, H. J., Barrett, G., & Starr, A. (1989). Brain potentials in a memory-
1023 scanning task. I. Modality and task effects on potentials to the
1024 probes. *Electroencephalography and Clinical Neurophysiology*, *72*(5), 407–421.
1025 https://doi.org/10.1016/0013-4694(89)90046-1

1026 Prosser S. (1995). Aspects of short-term auditory memory as revealed by a recognition task on
1027 multi-tone sequences. *Scandinavian Audiology*, *24*(4), 247–253.
1028 https://doi.org/10.3109/01050399509047544

1029 Roach, B. J., & Mathalon, D. H. (2008). Event-related EEG time-frequency analysis: an
1030 overview of measures and an analysis of early gamma band phase locking in
1031 schizophrenia. *Schizophrenia Bulletin*, *34*(5), 907–926.
1032 https://doi.org/10.1093/schbul/sbn093

1033 Rodieck, R. W. (1979). Visual pathways. *Annual Review of Neuroscience, 2,* 193–
1034 225. https://doi.org/10.1146/annurev.ne.02.030179.001205

1035 Rouder, J. N., Morey, R. D., Morey, C. C., & Cowan, N. (2011). How to measure working
1036 memory capacity in the change detection paradigm. *Psychonomic Bulletin &*
1037 *Review*, *18*(2), 324–330. https://doi.org/10.3758/s13423-011-0055-3

1038 Roux, F., & Uhlhaas, P. J. (2014). Working memory and neural oscillations: α-γ versus θ-γ
1039 codes for distinct WM information?. *Trends in Cognitive Sciences*, *18*(1), 16–25.
1040 https://doi.org/10.1016/j.tics.2013.10.010

1041 Schurgin M. W. (2018). Visual memory, the long and the short of it: A review of visual working
1042 memory and long-term memory. *Attention, Perception & Psychophysics*, *80*(5),
1043 1035–1056. https://doi.org/10.3758/s13414-018-1522-y

1044 Schwartz, I. R. (1992). The superior olivary complex and lateral lemniscal nuclei. In *The*
1045 *mammalian auditory pathway: neuroanatomy* (pp. 117-167). New York, NY: Springer
1046 New York.

1047 Scimeca, J. M., Kiyonaga, A., & D'Esposito, M. (2018). Reaffirming the sensory recruitment
1048 account of working memory. *Trends in Cognitive Sciences*, *22*(3), 190–192.
1049 https://doi.org/10.1016/j.tics.2017.12.007

1050 Silvanto, J., & Soto, D. (2012). Causal evidence for subliminal percept-to-memory interference
1051 in early visual cortex. *NeuroImage*, *59*(1), 840–845.
1052 https://doi.org/10.1016/j.neuroimage.2011.07.062

1053 Stokes M. G. (2015). 'Activity-silent' working memory in prefrontal cortex: a dynamic coding
1054 framework. *Trends in cognitive sciences,* *19*(7), 394–405.
1055 https://doi.org/10.1016/j.tics.2015.05.004

1056 Treder M. S. (2020). MVPA-Light: A Classification and Regression Toolbox for Multi-
1057 Dimensional Data. *Frontiers in Neuroscience*, *14*, 289.
1058 https://doi.org/10.3389/fnins.2020.00289

1059 Tuladhar, A. M., ter Huurne, N., Schoffelen, J. M., Maris, E., Oostenveld, R., & Jensen, O.
1060 (2007). Parieto-occipital sources account for the increase in alpha activity with working

memory load. *Human Brain Mapping*, *28*(8), 785–792. https://doi.org/10.1002/hbm.20306

Uluç, I., Schmidt, T. T., Wu, Y. H., & Blankenburg, F. (2018). Content-specific codes of parametric auditory working memory in humans. *NeuroImage*, *183*, 254–262. https://doi.org/10.1016/j.neuroimage.2018.08.024

van Ede, F., Chekroud, S. R., & Nobre, A. C. (2019). Human gaze tracks attentional focusing in memorized visual space. *Nature Human Behaviour,* *3*(5), 462–470. https://doi.org/10.1038/s41562-019-0549-y

van Dijk, H., Nieuwenhuis, I. L., & Jensen, O. (2010). Left temporal alpha band activity increases during working memory retention of pitches. *The European Journal of Neuroscience*, *31*(9), 1701–1707. https://doi.org/10.1111/j.1460-9568.2010.07227.x

Vogel, E. K., & Machizawa, M. G. (2004). Neural activity predicts individual differences in visual working memory capacity. *Nature*, *428*(6984), 748–751. https://doi.org/10.1038/nature02447

Wianda, E., & Ross, B. (2019). The roles of alpha oscillation in working memory retention. *Brain and Behavior*, *9*(4), e01263. https://doi.org/10.1002/brb3.1263

Williamson, V. J., Baddeley, A. D., & Hitch, G. J. (2010). Musicians' and nonmusicians' short-term memory for verbal and musical sequences: comparing phonological similarity and pitch proximity. *Memory & Cognition*, *38*(2), 163–175. https://doi.org/10.3758/MC.38.2.163

Wilsch, A., & Obleser, J. (2016). What works in auditory working memory? A neural oscillations perspective. *Brain Research*, *1640*, 193–207. https://doi.org/10.1016/j.brainres.2015.10.054

1084 Woldorff, M. G., Tempelmann, C., Fell, J., Tegeler, C., Gaschler-Markefski, B., Hinrichs, H.,
1085 Heinz, H. J., & Scheich, H. (1999). Lateralized auditory spatial perception and the
1086 contralaterality of cortical processing as studied with functional magnetic resonance
1087 imaging and magnetoencephalography. *Human Brain Mapping, 7*(1), 49–66.
1088 https://doi.org/10.1002/(SICI)1097-0193(1999)7:1<49::AID-HBM5>3.0.CO;2-J